Photodisintegration of Copper*

P. R. BYERLY, JR.,† AND W. E. STEPHENS
Department of Physics,‡ University of Pennsylvania, Philadelphia, Pennsylvania

(Received March 21, 1951)

The energy and angular distributions of the protons, deuterons, and alpha-particles and the energy distribution of neutrons emitted from copper nuclei irradiated with the x-rays from a 24-Mev betatron were determined with the use of photographic emulsions. The yields of neutrons, protons, deuterons, and alpha-particles were observed to be 3.6, 1.07, 0.34, and 0.04×10^6 particles, respectively, per mole per roentgen unit. A comparison of the neutron:proton yields and the energy distribution with the theoretical predictions of the statistical models and direct photoelectric action indicate that the photodisintegration of copper consists mainly in the evaporation of nuclear particles from the excited nuclei. However, the large numbers of deuterons observed can only be explained by a different mechanism such as the "pick up" of a proton by an emerging neutron. About 10 percent of the neutrons and protons have energies greater than expected from evaporation. These are ascribed to a direct photoelectric effect. The observed angular anisotropy of these high energy protons supports this interpretation.

I. INTRODUCTION

MEASUREMENTS[1] of photodisintegration cross sections in the middle weight nuclei, where the photoreaction leads to a radioactive isotope, indicate photoproton to photoneutron yield ratios considerably larger than theoretical calculations[2] based on the evaporation of nuclear particles from an excited nucleus. Explanations[3–5] for this discrepancy differ with regard to the details of the emitted particles. Initial observation from experiments[6] on the angle and energy distribution of the photoprotons from magnesium were consistent with an evaporation process. We then started to examine the photoneutrons from copper by proton recoils in nuclear emulsions. In the course of this work, it became evident that a large number of photoprotons were also being emitted. It proved possible to determine the numbers and energy distributions of both the neutrons and the charged particles emitted in the photonuclear process. Some results of these experiments have been published.[7] Meanwhile, other research has been published[8–10] which indicates the occurrence of direct photoelectric effects in nucleii. Several theoretical discussions of the photonuclear process have been published.[11,12]

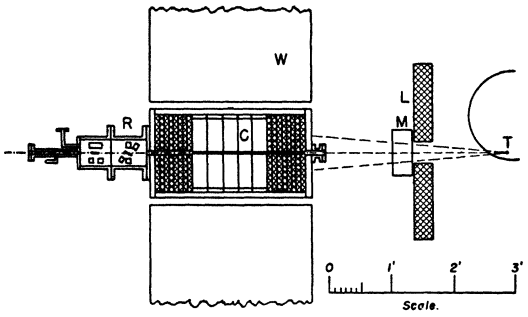

FIG. 1. Experimental arrangement showing betatron target T, lead wall L, monitor M, evacuated collimator C, concrete wall W, evacuated double camera T, foils F.

TABLE I. Details of various exposures.

Run	1	2a	2b	3	4
		Double proton camera			
Camera	Single proton	front section	rear section	Single proton	Neutron
Foil thickness (mg/cm²)	9.1	9.1	9.1	none	
Inches	0.0004	0.0004	0.0004		$\frac{1}{4}$
Angle to beam	0°	30°	0°		0°
Betatron energy	24 Mev	24	24	24	24
Roentgens at foil	8150	9125	9125	3800	8290
Emulsion	Ilford C-2	Ilford C-2	Ilford C-2 and NTC-3 Exp.	Ilford C-2	Ilford C-2
Thickness	100μ	200μ	200μ and 100μ	200μ	100μ
Size (in.)	$\frac{1}{4}\times1$	$\frac{1}{4}\times1$	$\frac{1}{4}\times1$ and 1×1	$\frac{1}{4}\times1$	1×3
Area scanned (mm²)	521	242 total	52	52	98
Distance from froil to start of scan (in.)	$\frac{1}{4}$	1	$\frac{3}{8}$	1	$1\frac{1}{8}$
Purpose	preliminary energy distribution	angular and energy distribution	grain counting	background	neutron energy
Total tracks measured	1000	1796	200	6	1000 recoils

* This paper contains essential portions of a thesis by P. R. Byerly, Jr., presented to the Faculty of the Graduate School of the University of Pennsylvania in partial fulfillment of the requirements for the Ph.D. degree.

† Now at the Radiation Laboratory, University of California, Berkeley, California.

‡ Supported in part by the joint program of the ONR and AEC; also aided by a grant from the Committee to Aid Research of the University of Pennsylvania.

[1] O. Hirzel and H. Wäffler, Helv. Phys. Acta **20**, 374 (1947).
[2] V. F. Weisskopf and D. H. Ewing, Phys. Rev. **57**, 472, 935 (1940).
[3] L. I. Schiff, Phys. Rev. **73**, 1311 (1948).
[4] E. D. Courant, Phys. Rev. **74**, 1226 A (1948); and private communication.
[5] P. Jensen, Naturwiss. **35**, 190 (1948).
[6] Toms, Halpern, and Stephens, Phys. Rev. **77**, 753 A (1950).
[7] P. R. Byerly, Jr. and W. E. Stephens, Phys. Rev. **81**, 473 (1951).
[8] B. C. Diven and G. M. Almy, Phys. Rev. **79**, 242 A (1950); **80**, 407 (1950).
[9] Curtis, Hornbostel, Lee, and Salant, Phys. Rev. **77**, 290 (1950).
[10] H. L. Poss, Phys. Rev. **79**, 539 (1950).
[11] M. Goldhaber and E. Teller, Phys. Rev. **74**, 1046 (1948).
[12] J. S. Levinger and H. A. Bethe, Phys. Rev. **78**, 115 (1950).

II. EXPERIMENTS

A. Detection of Deuterons

A collimated beam of x-rays from a 24-Mev betatron was used to irradiate targets of pure copper, and the photoparticles were observed in nuclear emulsions. The experimental arrangement is shown in Fig. 1. The setup was similar to that described previously[13] with the addition of a lead wall, L, and a concrete wall, W, to improve the shielding. The monitor, M, was calibrated against a 100 R Victoreen thimble chamber in a three-inch prestwood box for betatron energies from 15 Mev to 25 Mev. In order to check the alignment of the x-ray beam, the collimator, and the camera, plugs were made to hold x-ray film along the axis of the beam at the entrance and exit holes of the camera. Adjustments were made until the beam and apparatus were aligned to better than 1/64 in.

Preliminary runs with copper to look for neutron recoils in the emulsions had indicated an abundance of photoprotons from the copper. Then the first run was made to explore the energy distribution of these photoprotons. A foil of 0.4-mil copper (9.1 mg/cm^2) was placed at a small angle to the x-ray beam, and several Ilford C-2 nuclear emulsion plates, cut to $\frac{1}{2}$ in.$\times$1 in., were placed alongside the foil with their surfaces tangent to the bottom of the beam. (Table I gives the details of the various exposures.) Now 521 square mm of these plates were scanned for tracks that enter the surface of the emulsion and come from the foil. These tracks were required to have a dip angle between 0° and 15° and a horizontal angle of 90°$\pm$15° to the beam direction. Here 1000 tracks satisfied these criteria, and their lengths were measured.

About 20 percent of the otherwise good tracks did not end in the emulsion. To correct for these, the geometric probability that a track of a given length would go through the emulsion was calculated on the assumption that the protons were ejected uniformly in the irradiated portions of the foil. The observed tracks which did not leave the emulsion were corrected by this factor. Half the equivalent foil thickness was added to the observed range, and this total range changed to proton energy by the range-energy curve for Ilford emulsions.[14] Figure 2 gives the resulting energy distribution. The extra peak at 2.5 Mev and the low energy, 1.9 Mev, of the low energy protons appeared anomalous for copper.

In order to check the possibility that deuterons were producing these anomalies, a run (Table I, 2b) was arranged to allow grain counting on the tracks to identify the particle mass. The rear section of the double camera was used for the grain counting experiment. As in run 1, the copper foil was set at 0° to the beam, and the plates set close alongside. On one side

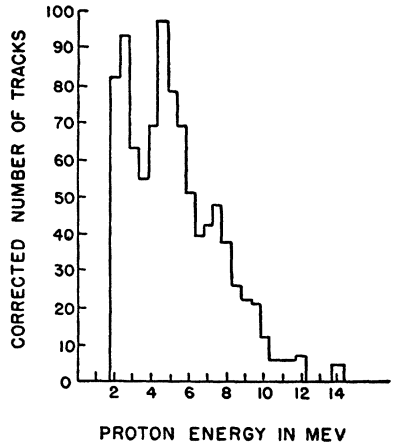

FIG. 2. Corrected energy distribution of photoprotons in run 1.

were set two, $\frac{1}{4}$-in.$\times$1-in., Ilford C-2, 200μ plates and on the other side, a 1-in.$\times$1-in., Eastman NTC-3 Exp., 100μ plate. Run number 2a using the front section of the camera was arranged to give an angular distribution of the protons at the same time. The emulsion thickness was increased to 200μ to reduce the probability that a long-range proton would go through the emulsion. In the front section of the double proton camera was mounted a 0.4-mil copper foil at an angle of 30° to the beam. Ten, $\frac{1}{4}$-in.$\times$1-in., Ilford C-2, 200μ nuclear plates were set at angles of 30°, 60°, 90°, 120°, and 150° to the beam. All the front corners were placed about $\frac{3}{8}$-in. from the axis of the $\frac{1}{4}$-in. diameter beam. The plates

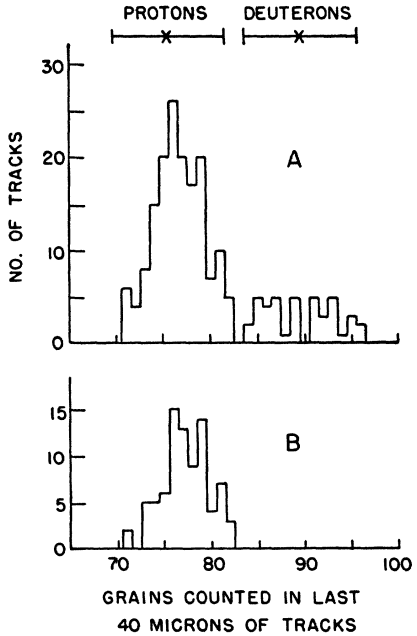

FIG. 3. A. Number of tracks entering surface (photoparticles) as a function of grains counted in the last 40μ of track. B. Number of tracks originating inside emulsion (recoil protons) as a functions of grains counted in last 40μ of track. Faded Ilford C-2 200μ emulsion (selected for flat tracks).

[13] M. E. Toms and W. E. Stephens, Phys. Rev. **82**, 709 (1951).
[14] Lattes, Fowler, and Cuer, Proc. Roy. Soc. (London) **59**, 883 (1947).

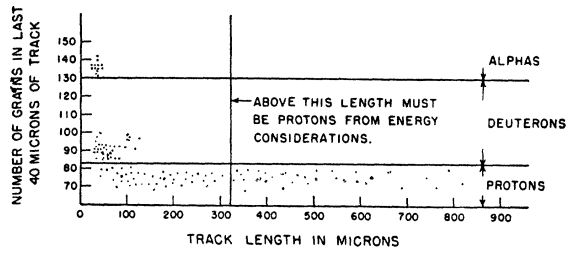

FIG. 4. Distribution of tracks in grain count and track length.

were aligned pointing to the foil and with their top surfaces tangent to the bottom of the beam. After an exposure of 9125 roentgens of 24-Mev bremsstrahlung x-rays in both sections of the camera, the plates were removed and processed. One of the rear section Ilford C-2 plates was allowed to fade for one week and then developed normally by a temperature change method. The second Ilford plate was developed immediately with an amidol-sodium sulfite developer. (25 grams sodium sulphite (anhydrous) plus 3 grams amidol to 1 liter of water instead of D-19.) The Eastman NTC-3 Exp. was developed strongly. All of these plates allowed grain counting on the proton tracks.

The faded Ilford plate was the most satisfactory, and Fig. 3 shows the numbers of tracks as a function of grains in the last 40μ of the track. Figure 3A shows the results of grain counting tracks which entered the surface of the emulsion in a direction from the foil, ended in the emulsion, and had small enough dip so that the last 40μ of the track were all in focus. This latter criterion was only to eliminate the need for a correction in grain spacing due to dip. Two groups of tracks are evident in Fig. 3A. One group has an average of 77 grains and is ascribed to protons. This identification is confirmed by similarly grain counting tracks which originated inside the emulsion and which must certainly have been recoil protons. Figure 3B shows the numbers of these recoil protons as a function of grains in the last 40μ, in agreement with the lower peak in Fig. 3A. The second group of tracks in Fig. 3A has an average of 90 grains in the last 40μ of track and is ascribed to deuterons. According to Lattes *et al.*,[15] the grain counts vary as the 0.289 power of the mass. This relation would predict a ratio of 1.22 for the grain count of deuterons compared to protons. The observed value of 1.17 seems in agreement with this.

As a check on this assignment, grain counting was also done on the amidol developed plate. Two groups were also evident with a grain count ratio of 1.26. The grain counts on the phototracks from the faded plate are plotted in Fig. 4 as a function of the track length. All tracks over 330μ must be protons from considerations of the maximum photon energy and the deuteron binding energy in copper. Also on this plot are a few tracks identified as alpha-particles because of their high grain count. The distinction between protons, deuterons, and alpha-particles is clearly evident. It also seems clear that most of the low energy peak of Fig. 2 is due to deuterons, as had been suspected.

Since it is possible that the selection of tracks on the criterion of flatness of the last 40μ of track might discriminate between protons and deuterons, the grain counting was repeated and all the phototracks in a selected region were counted for the number of grains in the last 10μ. These tracks were separated into protons and deuterons on the basis of this count. We found 149 protons and 46 deuterons, giving the ratio of protons to deuterons as 3.24 to 1 with an uncertainty of about 30 percent. The deuteron ranges were changed to an energy scale, and the distribution in energy is shown in the histogram of Fig. 5.

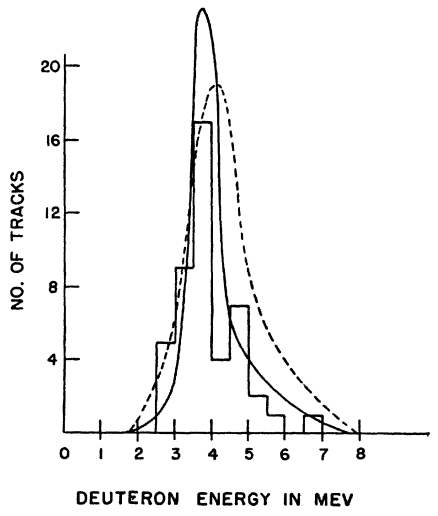

FIG. 5. Energy distribution of deuterons. The histogram indicates the observed tracks identified by grain counting as deuterons. The solid curve is the distribution calculated on the statistical model. The dashed curve is based on Schiff's model.

B. Protons and Neutrons

The angular distribution plates in the front section of the proton camera in exposure 2a were developed by temperature development in D-19. It was not found possible to avoid surface fogging in the development of these 200μ emulsions. Consequently, several grain layers were wiped off the emulsions with cotton after washing. This allowed the tracks to be followed to the surface and it is believed affects the true length by less than 1μ. Different areas were scanned on the 30°, 60°, 90°, 120°, and 150° plates, as shown in Table II. Since these areas were at different distances from the foil, the effective solid angles were measured by a separate experiment in which the copper foil was replaced by a similar polonium alpha-source. Similar nuclear emulsions were exposed and the alpha-particles counted in equivalent scanned areas. The source was calibrated in a flow counter and the solid angle determined for the regions scanned on the plates. The criteria for selection

[15] Lattes, Occhialini, and Powell, Proc. Phys. Soc. (London) **61**, 173 (1948).

TABLE II. Angular distribution of tracks in run 2a.

Angle	Area scanned (mm^2)	Solid angle per mm^2	Tracks observed	Correction factor	Corrected number
30°	86	1.65×10^{-6}	175	3.35	586
60°	39	10.5×10^{-6}	423	1.17	495
90° right	26	9.2×10^{-6}	270	1	559
90° left	26	9.2×10^{-6}	289		
120°	39	10.5×10^{-6}	481	1.17	564
150°	86	1.65×10^{-6}	158	3.35	530

of tracks were: track must start on the surface of the emulsion and end in the emulsion; the initial direction must be from the foil both in horizontal angle (±7°) and dip (0° to 15°). The measured range of the track was increased by the equivalent half-thickness of the foil (13μ to 15μ). This is also the uncertainty in energy of the particles and varies from ±⅓ Mev for 3-Mev protons to ±0.15 Mev for 10-Mev protons.

Figure 6 shows the observed numbers of tracks, corrected for solid angle scanned, plotted as a function of angle. In addition to the totals, the angular distribution is given for groups of energies: 1.6 to 3.6 Mev (which is mostly deuterons), 3.6 to 10 Mev, and above 10 Mev. In order to avoid any distortion, the "above 10 Mev" group includes also the 33 tracks which did not end in the emulsion. These were all over 10 Mev, so no correction of length was necessary.

The energy distribution of the tracks measured in the angular distribution is shown in Fig. 7. The energy distributions observed at separate angles are similar but less significant statistically. The energy distributions observed on opposite 90° plates are quite similar and check the alignment of the beam, foil, and plates.

The background was determined in several ways. Run number 3 was similar to the front section of run 2 with the foil omitted. Only six tracks were observed at 90°. This corresponds to 15 out of the 559 tracks observed at 90° in run 2 or to 2.7 percent. In run 2, all the tracks entering the surface of the emulsions in the wrong direction were plotted as a function of angle from the foil direction. They were quite isotropic and if ascribed to protons scattered from the walls would give an additional correction of 8 out of 1796 or 0.6 percent. The tracks that went through the emulsion were 1.8 percent. Consequently, the total correction is negligible except for the high energy portion of the spectrum.

In order to check the possibility of an (n,p) reaction producing protons by the background neutrons in the x-ray beam, we attempted to activate phosphorus in the collimated beam at the same time a copper foil was activated. No activity was detected in the phosphorus when copper was activated to 500 counts per second. From this we deduce less than 0.1 percent of the protons are from an (n,p) reaction.

In run 2 a large number of alpha-particles were observed and measured. Although many of these are

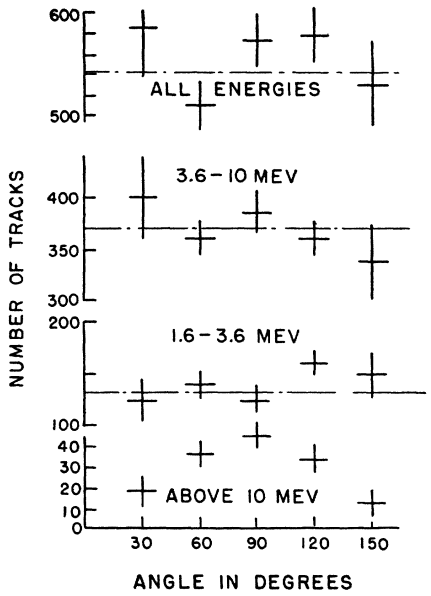

FIG. 6. Angular distribution of tracks for various energy groups.

contamination alpha-particles, when they were plotted against angle about the acceptable direction from the foil, as in Fig. 8, a surplus was evident in the acceptable direction. These alpha-particles appear at all angles from the beam and are isotropic although the statistical uncertainty is as great as 30 percent at 30° and 150°. The energy distribution of these photo alpha-particles is given in Fig. 9. The ratio of the numbers of alpha-particles to protons is 1 to 24.3.

In run 4 a smaller camera was substituted for the proton camera. In this neutron camera, the target was a copper slug ¼ in. in diameter and ¼ in. long. Neutrons ejected from the copper were detected by proton recoils in nuclear emulsions placed nearby. The 1-in.×3-in., Ilford C-2, 100μ plates were set in a plane perpendicular to the beam with the leading edge ⅜ in. from the center of the copper. Proton recoils were measured which had

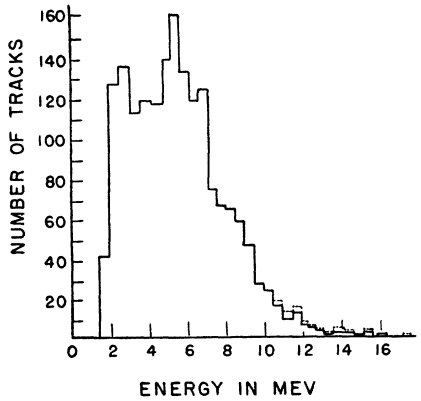

FIG. 7. Energy distribution of tracks measured at all angles. The dotted lines indicate those tracks which passed out of the emulsion.

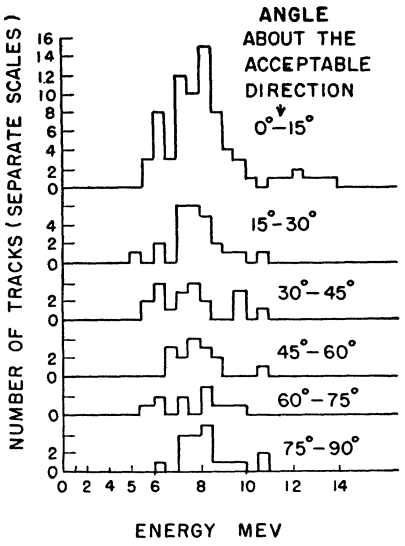

FIG. 8. Energy distribution of total alpha-particles as a function of angle from the acceptable direction.

angles within $\pm 15°$ to the direction from the center of the copper. The procedure described by Richards[16] was followed in making geometric corrections for wall effects, acceptance ratios, etc. Run number 3 was used for background determination. There were too few recoils in the acceptable direction in run 3 to give good statistics, so all the recoils were measured and a background estimated for run 4. Table III shows the background and observed good recoils. Figure 10 gives the energy distribution of the good neutron recoils corrected for background, acceptance ratios, and neutron-proton scattering cross section. This plot, then, should give the energy distribution of the photoneutrons emitted from the copper. Because of the presence of occasional clusters of background developed grains, tracks shorter than 3μ were not measured. This puts a lower limit of 0.3 Mev to the neutron energy detected.

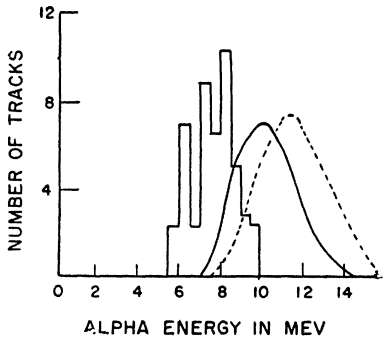

FIG. 9. Energy distribution of alpha-particles. The histogram gives the alpha-tracks ascribed to photodisintegration of copper. The solid curve is calculated on the statistical model. The dashed curve is calculated on Schiff's model.

[16] H. T. Richards, Phys. Rev. **59**, 796 (1941).

TABLE III. Neutron recoils and background.

Energy interval (Mev)	Recoils observed in run 3	Calculated background for run 4	Good recoils observed in run 4
0.3 to 0.8	75	60	236
0.8 to 1.3	51	41	286
1.3 to 1.8	26	21	166
1.8 to 2.3	7	5	96
greater than 2.3	5	4	216

C. Yields

The yields of the protons, deuterons, and alpha-particles could be determined from the solid angles and tracks observed. The neutron yields were determined both from the number of proton recoils and also by the radioactivity produced in the (γ,n) reactions. The yield of photoparticles is defined as

$$Y=Ly=nL/ANtR\omega,$$

where n is the number of photoparticles observed in an area "a" which subtends a solid angle ω at the foil, A is the area of the beam which intercepts the foil, N is the number of nuclei/cc, t is the thickness of the foil in the direction of the beam, R is the number of roentgen units delivered at the foil, ω is the fractional solid angle which the scanned area subtends at the foil, y is the yield per nucleus per roentgen unit, L is Avogadro's number, and Y is the yield per mole per roentgen unit.

In run number 2a at 90°, $R=9125$ roentgens, $Nt=1.72\times10^{20}$ nuclei/cm^2 in direction of beam, $A=0.317$ cm^2, $\omega=4.78\times10^{-4}$ for 52 mm^2 scanned and $n=559$ tracks observed in 52 mm^2 scanned, giving $Y=1.41\times10^6$ particles per mole roentgen unit. Since this includes both protons and deuterons, we can separate this into $Y_p=1.07\times10^6$ protons/mole/r and $Y_d=0.34\times10^6$ deuterons/mole/r.

In run number 4

$$n/\omega=n'/\sigma'N't'\omega k.$$

Here n is the number of neutrons entering the region in emulsion scanned for recoil protons, n' is the observed number of "good" recoil protons, σ' is the n-p scattering cross section, N' is the number of hydrogen nuclei/cc in the emulsion, t' is the distance along the neutron path in the scanned region, ω is the fractional solid angle subtended by the region scanned at the copper slug, and k is the fraction of recoils observed as "good" recoils (for $\pm 15°$). Then $N'=3.38\times10^{22}$ hydrogen nuclei/cc, $t'\omega=1.01\times10^{-4}$ for 98 mm^2 scanned of 100μ emulsion, $k=0.087$, and $n'/\sigma'=300\times10^{24}$ averaged over the energy spectrum, giving $n/\omega=1.0\times10^9$ neutrons; and $A=0.317$ cm^2, $Nt=5.35\times10^{22}$ copper nuclei/cm^2 in $\frac{1}{4}$-in. slug, $R=8290$ roentgen units, giving $y_n=0.70\times10^{-17}$ neutrons/nucleus/r or $Y_n=4.2\times10^6$ neutrons/mole/r.

This value is uncertain mainly due to the difficulty of selecting recoils within exactly the $\pm 15°$ angle. In

order to determine this neutron yield independently, we have measured the radioactivity produced in the $Cu^{65}(\gamma,n)Cu^{64}$ and $Cu^{63}(\gamma,n)Cu^{62}$ transmutations. During run 2, an 8-mil copper foil was activated at the exit of the double camera for three hours of the run. This foil was counted for several days, and the saturated activities of Cu^{62} and Cu^{64} were determined as 6900 counts/min and 550 counts/min. The counter was calibrated against a radium D plus E source[17] which determined the saturated disintegrations per minute of Cu^{62} to be 3.12×10^4 and of Cu^{64} to be 2.98×10^4. Using other data from run 2 gives $Y_{63}=2.6\times10^6$ neutron/mole of Cu^{63}/r and $Y_{65}=5.8\times10^6$ n/mole of Cu^{65}/r, combining to give $Y_n=3.56\times10^6$ neutrons/mole of copper/r. In addition, the excitation curve of Cu^{62} was taken by varying the betatron energy and observing the radioactivity produced. The cross-section curve was calculated from this excitation curve and the x-ray photon energy distribution.[18] A peak cross section of 0.10 barn was observed at 17.5 Mev, as shown in Fig. 11.

III. DISCUSSION

The yields of photoparticles from copper with 24-Mev x-rays can be summarized as:

$Y_p=1.07\times10^6$ protons/mole/r,
$Y_d=0.34\times10^6$ deuterons/mole/r,
$Y_\alpha=0.04\times10^6$ alphas/mole/r,
$Y_n=3.56\times10^6$ neutrons/mole/r from radioactivity,
or $=4.2\times10^6$ neutrons/mole/r from recoils.

The uncertainties in these yields is of the order of 50 percent. The relative values are perhaps somewhat better.

The proton yield is in good agreement with results of Mann and Halpern who give 1×10^6 protons/mole/r from copper in their scintillation detector survey.[19] The photoemission of protons has also been observed by Chastel[20] with the lithium gamma-rays. His cross section of 10^{-27} cm^2 is somewhat lower than the value inferred from our work. From the radioactivity produced and the threshold (γ,d) and (γ,α) reactions have been observed by the Saskatchewan group.[21] Their integrated cross sections for $S^{32}(\gamma,d)$ and $Rb^{87}(\gamma,\alpha)$ are somewhat lower than the values inferred from our yields. There are a number of values of the yields of (γn) reactions in copper. Price and Kerst[22] measured the total neutron yield by slowing the neutrons down and absorbing them in rhodium. Their value of 2.5×10^6 neutrons/mole/r is for 22-Mev x-rays. Estimating it to 2.8×10^6 n/M/r at 24 Mev still leaves it appreciably smaller than our value. However, the Saskatchewan group[21] has carefully measured the radioactivity produced, and from their results a yield of $.375\times10^6$ n/M/r can be calculated. These results on Cu^{63} are confirmed by Rosenfeld, Marshall, and Wright,[23] and others.[8,24]

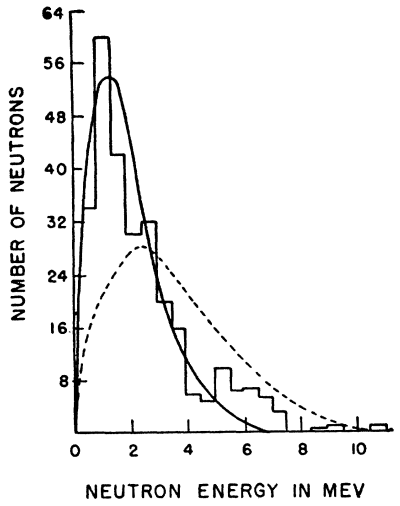

FIG. 10. Energy distribution of the neutrons. The histogram shows the distribution of recoil proton tracks corrected for background, acceptance ratio, and n-p cross section to give photoneutron energy distribution. The solid curve is calculated on the statistical model. The dashed curve is calculated on Schiff's model.

If we take $Y_n=3.8\times10^6$ n/M/r and add the others, we get a total photoyield of 5.24×10^6 particles/M/r or 8.7×10^{-18} particles/nucleus/r. This can be changed to an integrated cross section with reasonable assumptions as to shape of the cross-section curves. The total integrated cross section is estimated to be 1.4 Mev-barns. This can be compared with the value predicted by Goldhaber and Teller[11] of 0.91 Mev-barn. Levinger and Bethe[12] calculate a total integrated cross section

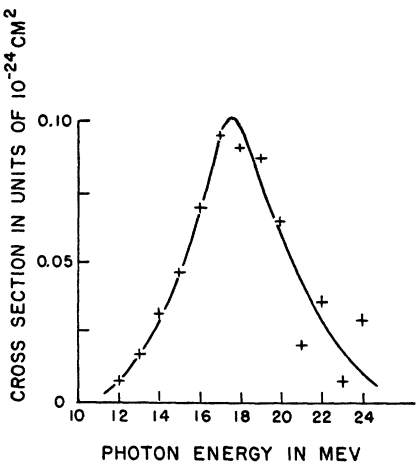

FIG. 11. Calculated cross section for $Cu^{63}(\gamma,n)Cu^{62}$ determined from the excitation curve of Cu^{62}.

[17] B. P. Burtt, Nucleonics **5**, No. 8, 28 (1949).
[18] Johns, Katz, Douglas, and Haslam, Phys. Rev. **80**, 1062 (1950).
[19] A. K. Mann and J. Halpern, Phys. Rev. **81**, 318 A (1951).
[20] R. Chastel, Compt. rend. **230**, 2020 (1950).
[21] Harrington, Katz, Haslam, and Johns, Phys. Rev. **81**, 660 A (1951); R. N. H. Haslam and H. M. Skarsgard, Phys. Rev. **81**, 479 L (1951).
[22] G. A. Price and D. W. Kerst, Phys. Rev. **77**, 806 (1950).
[23] Rosenfeld, Marshall, and Wright, Phys. Rev. **82**, 301A (1951).
[24] A. C. Helmholz and K. Strauch, Phys. Rev. **78**, 86 (1950).

for a more general dipole interaction and include the effect of exchange forces. Using a Yukawa well, $r_0=1.5\times10^{-13}$ cm, and a fraction of exchange force of $\frac{1}{2}$, they would calculate 1.32 Mev-barns for copper.

In order to compare the experimental results with theory in more detail, we have calculated both the energy distributions to be expected of the neutrons, protons, deuterons, and alphas, and also the relative yields expected on the various nuclear models. Since we do not know the cross-section curves for each transmutation nor the total photon absorption, we start from the experimental (γ,n) cross-section curves. On the basis of the statistical model nucleus of Weisskopf and Ewing,[2] we can then calculate the number and energy distribution of the evaporated protons, deuterons, and alphas. We have done these separately, normalizing the energy distribution curves to the

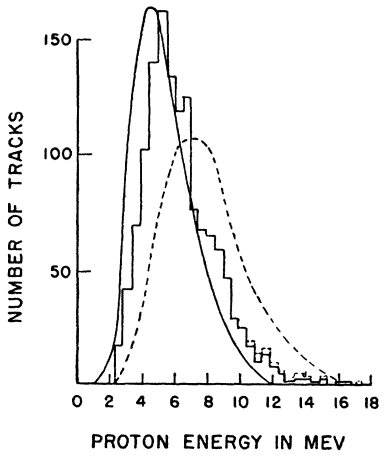

FIG. 12. Energy distribution of the photoprotons. The histogram represents the experimental results from run 2a with the deuterons subtracted. The dotted lines indicate those tracks which did not end in the emulsion. The solid curve is the normalized statistical model prediction and the dashed curve is the Schiff model.

experimental ones, so that the distribution comparison with experiment need not depend upon accurate yield data and vice versa. We have also considered the regular level excitation model proposed by Schiff[3] and the direct photoelectric interaction suggested by Courant.[4]

Almy and Diven[8] have written down the formula for the energy distribution $F(e)$ of a particle b evaporated from a nucleus with an energy e.

$$F(e)=eS_b(e)\int_0^{E_{\max}} K\omega_R(E-B_b-e)dE,$$

where e is the energy of an emitted particle b, $S_b(e)$ is the penetration factor,[2] ω_R is the level density of the resultant nucleus, E is the photon energy, B_b is the binding energy of the particle b; and

$$K=N(E,E_{\max})\sigma(\gamma,n)/C,$$

$$C=\int_0^{e_{n\,\max}} e_n\omega_R(E-B_n-e_n)de_n,$$

where N is the number of photons of energy E, σ is the (γ,n) cross section as a function of E, e_n is the emitted neutron energy, B_n is the neutron binding energy, and $e_{n\,\max}=E-B_n$. The total emission of particle b is the integral of F with respect to e from 0 to $e_{\max}=E-B_b$. The level density can be described by the normal statistical model[2] as

$$\omega_R(\mathcal{E})=\exp(a\mathcal{E})^{\frac{1}{2}} \quad \text{with} \quad a=1.6(A-40)^{\frac{1}{2}}$$

or by Schiff's regular level excitation[3]

$$\omega_R(\mathcal{E})=(a/4)\ln(a\mathcal{E}/4+1).$$

The coefficient C can be calculated from these to be

$$C_{WE}=(2/a)[(D-6/a)+\exp(aD)^{\frac{1}{2}}\times\{2(D+3/a)-(6/a)(aD)^{\frac{1}{2}}\}],$$

$$C_S=(a/8)(D+4/a)^2[\ln2(D+4/a)-3/2]+(D+3/a),$$

where $D=E-B$, and $\mathcal{E}=E-B_b-e$. The bremsstrahlung distribution N was taken from the calculations of the Saskatchewan group.[18] The binding energies were calculated from the empirical mass equation, checked with experimental values where possible, and are shown in Table IV. The (γ,n) cross section for Cu^{63} was taken from Fig. 11 and is close to the Saskatchewan curve.[18] The $Cu^{65}(\gamma,n)$ cross-section curve was assumed to be similar in magnitude but shifted down 0.7 Mev. This is somewhat different from the Saskatchewan curve,[18] which was not available at the time the calculations were made. A partial recalculation using the Saskatchewan curve does not materially change the values.

The energy distribution $F(e)$ was calculated for each level density formula and for each isotope of copper. The isotopic curves were combined and normalized to the experimental curves. Figures 10, 12, 5, and 9 show the comparison between the observed energy distributions of the neutrons, protons, deuterons, and alpha-particles, and the calculated distributions. In each case the histogram shows the experimental results, the solid curve represents the statistical model, and the dashed curve gives the results of Schiff's assumptions (also normalized to the observed number). Table V gives the results of integrating the energy distributions to get total calculated yields.

The agreement between experiment and the statistical model for the evaporation of neutrons seems quite good (Fig. 10 and Table V). There are, however, about 10 percent of the neutrons which have energies higher than expected on the Weisskopf and Ewing evaporation model.

It is possible that a larger energy level density at low excitations of the resultant nucleus, or an effect similar to Schiff's proposed selective excitation, might account for some of this discrepancy. However, in view of the fact that a similar high energy excess appears in the proton energy distribution curve, Fig. 12, and that these high energy protons have a non-isotropic distribution with a maximum at 90°, Fig. 6, it seems probable that these high energy neutrons and protons are the result of a direct photoelectric effect of a photon on a nucleon. These results are in good agreement with similar data for the photoprotons from silver reported by Almy and Diven.[8]

None of the theoretical calculations of the photon interaction have, so far, been extended to the calculation of these details. However, it would seem that a process of absorption of the photon by a nucleon, such as the dipole interaction discussed by Levinger and Bethe, could result in most of the observed phenomena. In a few cases the proton or neutron which has absorbed the photon could escape from the nucleus without further interaction, especially if the proton or neutron were on the surface. These particles would retain the photon energy minus the binding energy and would have a non-isotropic distribution with a maximum at 90° if they had no angular momentum in the nucleus.[4] Those particles which absorb a photon and make a collision within the nucleus might be expected to make further collisions and lose the absorbed energy to the nucleus as a whole. This excited nucleus would then evaporate a neutron or proton according to the statistical model. Although the number of directly ejected protons may be only a small fraction of the photon absorption and consequently difficult to observe in low atomic number elements where the low coulomb barrier permits appreciable proton evaporation in competition with neutron evaporation, it may nevertheless be a major fraction of the photoprotons from higher atomic number elements. Here the high coulomb barrier prevents appreciable proton evaporation in competition with neutron evaporation. Consequently, such a direct ejection of protons may account for the observation in heavy elements of larger (γ,p) cross sections than predicted by evaporation models.

The theoretical calculations on the statistical model seem to predict a larger number of low energy protons than were observed in Fig. 12. Since the neutron curves show good agreement in the low energy region, the discrepancy may be ascribed either to experimental error (the low energy shape was determined by subtracting the deuterons from the total curve, Fig. 7, and is uncertain due to the small numbers involved) or to errors in the coulomb barrier penetration factors.

The alpha-particles observed seem most probably to be evaporated from the compound nucleus (Fig. 9 and Table V). It seems reasonable to account for any discrepancies in numbers or energy between theory and experiment on the basis of some uncertainty in the experimental results, caused by the small numbers, and some uncertainty in the theoretical calculations. However, the alphas ejected in cosmic-ray stars are also of lower energy than expected.[25]

TABLE IV. Particle binding energies in copper.

	Cu^{63}		Cu^{65}	
	Calc. (Mev)	Exp. (Mev)	Calc. (Mev)	Exp. (Mev)
neutron	11.0	10.9	10.1	10.2
proton	6.1	6.2*	7.4	7.7*
deuteron	14.6		14.7	
alpha-particle	6.3		5.7	

* Determined from (γ,n) threshold and beta-ray energy.

None of these concepts, however, seem able to account for the large numbers of deuterons observed. All of the evaporation models predict several orders of magnitude too small a yield for evaporated deuterons (assuming preformed deuterons), despite the facts that the energy spectrum is consistent with a statistical model evaporation and that the angular distribution (as evidenced by the 1.6- to 3.6-Mev group in Fig. 6) seems isotropic. A calculation of the direct photoelectric[4] yield of preformed deuterons also gives much too small a number. Consequently, we are forced to postulate some other mechanism for this effect. The "pick-up" process[25] by which an outgoing "evaporated" neutron or proton picks up an apposite particle seems likely. In fact, the probability that an outgoing particle with velocity corresponding to its excitation temperature will happen to find another particle going in a similar direction with a similar velocity might be greater for these energies than for the high energies Chew and Goldberger[26] consider. On the other hand, it will be less probable that this "deuteron" will escape over the barrier at these lower energies. York[27] has observed that 1/12 of the 90-Mev neutrons which interacted

TABLE V. Relative yields of photoparticles (in units of 10^6 particles/mole/r).

	Neutrons	Protons	Deuterons	Alphas
Observed				
Cu^{63}	2.6			
Cu^{65}	5.8			
Normal copper	3.6	1.07	0.34	0.04
Calculated with statistical model of Weisskopf and Ewing				
Cu^{63}	(3.0)*	1.07	0.0002	
Cu^{65}	(5.6)*	0.37	0.0005	
Normal copper	(3.8)*	0.86	0.0003	0.006
Calculated with Schiff model				
Normal copper	(3.6)*	2.0	0.0013	0.040
Calculated with formulae of Le Couteur				
Normal copper	(3.6)*	1.1	0.0023	0.015

* Assumed values.

[25] Bernardini, Cortini, and Manfredini, Phys. Rev. **79**, 952 (1950).
[26] G. F. Chew and M. L. Goldberger, Phys. Rev. **77**, 470 (1950).
[27] H. York, Phys. Rev. **75**, 1467 A (1949).

with a carbon nucleus "picked up" a proton and escaped as a deuteron. The present observation of 1/14 as many deuterons as neutrons and protons may be the result of such a "pick-up" process at low energies. If this interpretation were true, one might expect to observe a few tritons also emerging from copper. However, the binding energy of a triton to its residual nucleus is large, so that its probability of escape would be small.

Some of the initial photographic techniques and the nuclear emulsion camera used in this work were developed by Miss M. Elaine Toms.

PHYSICAL REVIEW VOLUME 83, NUMBER 1 JULY 1, 1951

The Radiations from Hafnium

S. B. BURSON, K. W. BLAIR, H. B. KELLER, AND S. WEXLER
Argonne National Laboratory, Chicago, Illinois
(Received March 12, 1951)

The 70-day, 45-day, 5.5-hour, and 19-second activities of Hf have been investigated by spectrometric, spectrographic, absorption, and coincidence methods. From activation experiments on the separated Hf isotopes, the following assignments have been made: 70-day—$_{72}Hf^{175}$; 19-second—$_{72}Hf^{179*}$; 5.5-hour—$_{72}Hf^{180*}$; 45-day—$_{72}Hf^{181}$.

70-day period.—The photographic spectrograms of the internal conversion electrons associated with the 70-day period in $_{72}Hf^{175}$ indicated the presence of four gamma-rays. The association of Lu work functions with the various lines confirmed the hypothesis of K electron capture in $_{72}Hf^{175}$ leading to an excited state of $_{71}Lu^{175}$.

45-day period.—An investigation of the internal conversion electron spectrum in the Argonne 180° beta-ray spectrometer indicated the presence of one beta-ray of 0.42±0.01 Mev and five gamma-rays. An upper limit of 1 percent may be placed on any more energetic beta-ray. Single and coincidence absorptions in lead and aluminum showed the three strongest gamma-rays and the single beta-ray. Delayed coincidence absorption indicated that the 0.42-Mev beta-ray leads directly to the 22-microsecond metastable state of $_{73}Ta^{181}$. No delayed gamma-coincidences were found. Thus, all gamma-rays appear to follow the 22-microsecond state. Additional coincidence measurements showed internal conversion electron groups corresponding to three of the gamma-rays. The decay scheme proposed by Chu and Wiedenbeck, as modified by Cork *et al.* was confirmed.

5.5-hour period.—Activation of extremely pure Hf samples showed an activity of 5.5 hours in addition to the 45-day period. The assignment of this activity to Hf was confirmed by chemical methods. No delayed coincidences were observed. Internal conversion electron groups corresponding to five gamma-rays were resolved; absorption in lead indicated three of the photon components. Aluminum absorptions indicated coincidences between internal conversion electron groups from at least two of the gamma-rays. Activation of separated isotopes shows that this activity is one of an isomeric state of $_{72}Hf^{180}$.

19-second period.—A photographic spectrogram of the internal conversion electrons showed the presence of a single gamma-ray; the association of Hf work functions with the four lines observed verified the hypothesis of an isomeric state in $_{72}Hf^{179}$.

INTRODUCTION

EXTENSIVE experiments have been carried out by several investigators[1–15] on the 45-day activity of $_{72}Hf^{181}$. A longer activity of 70 days has also been reported[16] and assigned to $_{72}Hf^{175}$. The results of the spectrographic measurements are generally in good agreement; but many of the coincidence measurements seem to be in conflict and at times have led to anomalous conclusions. The high intensity of the internal conversion electron groups from the many gamma-rays present make the interpretation of both single and coincidence absorption curves extremely difficult. We have taken advantage of the 22-microsecond isomeric state of $_{73}Ta^{181}$ to separate the primary beta-ray from the internal conversion electron spectrum, thereby facilitating careful inspection of each independently.

After the completion of many of these experiments using normal Hf, the separated isotopes were obtained from the Isotopes Division of the Oak Ridge National Laboratory. In the subsequent discussion, all references to Hf indicate normal Hf, the separated isotopes being referred to explicitly. These isotopes made possible the definite isotopic assignment of the activities. Accurate gamma-ray energy determinations were made by measurement of the internal conversion electron groups associated with each isotope. The details of the techniques and instrumentation employed in these measurements will be discussed in a subsequent publication.[17]

[1] H. Neuert, Z. Naturforsch. **2a**, 432 (1947).
[2] L. Madansky and M. L. Wiedenbeck, Phys. Rev. **72**, 185 (1947).
[3] M. L. Wiedenbeck and K. Y. Chu, Phys. Rev. **72**, 1164 (1947).
[4] S. DeBenedetti and F. K. McGowan, Phys. Rev. **74**, 728 (1948); Phys. Rev. **70**, 569 (1946).
[5] Cork, Schreffler, and Fowler, Phys. Rev. **72**, 1209 (1947).
[6] Bunyan, Lundby, Ward, and Walker, Proc. Phys. Soc. (London) **61**, 300 (1948).
[7] Benes, Ghosh, Hedgran, and Hole, Nature **162**, 261 (1948).
[8] A. F. Voight and B. J. Thamer, Phys. Rev. **74**, 1264 (1948).
[9] Mandeville, Scherb, and Keighton, Phys. Rev. **75**, 221 (1949).
[10] K. Y. Chu and M. L. Wiedenbeck, Phys. Rev. **75**, 226 (1949).
[11] Arne Lundby, Phys. Rev. **76**, 1809 (1949).
[12] Erling Jensen, Phys. Rev. **76**, 958 (1949).
[13] Cork, Stoddard, Rutledge, Branyan, and LeBlanc, Phys. Rev. **78**, 299 (1950).
[14] M. Deutsch and A. Hedgran, Phys. Rev. **79**, 400 (1950).
[15] W. C. Barber, Phys. Rev. **78**, 641 (1950).
[16] G. Wilkinson and H. Hicks, Phys. Rev. **75**, 696 (1949).
[17] H. B. Keller and J. M. Cork, to be published.